0026-895X/00/020279-09$3.00/0
MOLECULAR PHARMACOLOGY

MOL 58:279–287, 2000 /13197/842487

CYP2C40, a Unique Arachidonic Acid 16-Hydroxylase, Is the Major CYP2C in Murine Intestinal Tract

CHENG-CHUNG TSAO, JULIE FOLEY, SHERRY J. COULTER, ROBERT MARONPOT, DARRYL C. ZELDIN, and JOYCE A. GOLDSTEIN

Laboratory of Pharmacology and Chemistry (C.-C.T, S.J.C., J.A.G.), Laboratory of Experimental Pathology (J.F., R.M.), and Laboratory of Pulmonary Pathobiology (D.C.Z.), National Institute of Environmental Health Sciences, Research Triangle Park, North Carolina

Received for publication December 28, 1999; accepted May 17, 2000

This paper is available online at http://www.molpharm.org

ABSTRACT

We recently identified five different murine CYP2C cDNAs from a murine cDNA library. When expressed in a bacterial cDNA expression system, all five recombinant proteins metabolized arachidonic acid but produced distinctly different profiles. In addition, some CYP2C mRNAs were found in extrahepatic tissues, as well as in liver. Immunoblots with an antibody raised against recombinant CYP2C38, which recognizes all five murine CYP2Cs, demonstrated that among extrahepatic tissues, colon and cecum contained the highest amount of CYP2Cs. The highest concentration of CYP2Cs occurred in cecum and colon (cecum $\geq$ proximal colon $\gg$ distal colon), with lower levels in duodenum, jejunum, and ileum. Immunohistochemical studies revealed that CYP2Cs were localized principally in epithelial cells and autonomic ganglia in gut and colon. Polymerase chain reaction amplification of reverse-transcribed mRNA using murine CYP2C-specific primers followed by cloning and sequencing identified CYP2C40 as the major CYP2C isoform expressed in murine intestinal tract. Recombinant CYP2C40 metabolized arachidonic acid in a regio- and stereospecific manner to 16(*R*)-HETE (hydroxyeicosatetraenoic acid) as the major product. To our knowledge, CYP2C40 is the first enzyme known to produce primarily 16-HETE. We conclude that CYP2C40 is one of the major cytochrome P450 proteins in the mouse intestinal tract. In the light of vasoactive and anti-neutrophilic effects of 16-HETE, we hypothesize that CYP2C40 may play an important role in endogenous biological functions in intestine.

Intestinal cytochrome P450 (CYP) enzymes are proposed to be involved in the biotransformation of ingested xenobiotics and the activation/detoxification of toxicants and procarcinogens (Kaminsky and Fasco, 1992). Although many CYP proteins are found constitutively in the intestinal tract, the endogenous functions of these enzymes are still not clear. A number of CYP proteins constitutively expressed in the gastrointestinal tract of humans and rats include members of the CYP1A, CYP2C, CYP2D, CYP2E, CYP2J, and CYP3A subfamilies (Murray et al., 1988; Peters et al., 1989; Rich et al., 1989; de Waziers et al., 1990; Shimizu et al., 1990; Fasco et al., 1993; Zeldin et al., 1997; Zhang et al., 1998; Dey et al., 1999). These CYP proteins are differentially expressed in various regions of the gastrointestinal tract. Most CYP proteins are highest in the duodenum, although concentrations decrease distally (Peters et al., 1989; de Waziers et al., 1990; Shimizu et al., 1990; Kaminsky and Fasco, 1992; Zhang et al., 1998; Dey et al., 1999), but some are expressed at similar concentrations throughout the intestinal tract (Zeldin et al., 1997). Immunohistochemical and in situ hybridization studies have demonstrated that CYP enzymes are expressed in different cell types in these tissues, including columnar epithelial cells, enterocytes, smooth muscle cells, and vascular endothelium (Murray et al., 1988; Peters et al., 1989; Shimizu et al., 1990; Zeldin et al., 1997; Zhang et al., 1998; Dey et al., 1999).

Among the endogenous functions of intestinal CYP proteins, many of these enzymes are capable of metabolizing arachidonic acid (AA) to a variety of biologically active eicosanoids (Macica et al., 1993; Zeldin et al., 1997). In the presence of NADPH and molecular oxygen, CYPs can metabolize AA to several oxygenated metabolites including: 1) four regioisomeric epoxyeicosatrienoic acids (EETs) (5,6-, 8,9-, 11,12-, and 14,15-EET), each of which can be hydrolyzed by epoxide hydrolases to corresponding dihydroxyeicosatrienoic acids; 2) six regioisomeric *cis*-trans conjugated monohydroxyeicosatetraenoic acids (HETEs); and 3) *o*-terminal alcohols (20-HETE and 19-HETE) (Capdevila et al., 1981, 1992; Oliw et al., 1982). It has been shown that intestinal microsomal fractions metabolize AA to several regioisomeric EETs and HETEs, and these compounds have been shown to exert effects on intestinal motility, secretion, and blood flow (Whittle and Vane, 1989; Zeldin et al., 1997). Furthermore, CYP-AA metabolites possess a diversity of biological proper-

ABBREVIATIONS: CYP, cytochrome P450; AA, arachidonic acid; EET, epoxyeicosatetraenoic acid; HETE, hydroxyeicosatetraenoic acid; HPLC, high performance liquid chromatography; PCR, polymerase chain reaction; RT-PCR, reverse transcriptase PCR; PI, phosphatidylinositol.

ties that can influence cell function. For example, 5,6- and 14,15-EETs have been reported to act as intestinal and renal vasodilators (Proctor et al., 1987; McGiff, 1991). In addition to regioselective biological activities, EETs and HETEs exhibit stereoselective activity. It has been found that the (*S*) enantiomers of 16- and 17-HETEs inhibit proximal tubule ATPase activity, whereas their (*R*) isomers have negligible effects (Carroll et al., 1996). In contrast, 16(*R*)-HETE causes vasodilation, whereas 16(*S*)-HETE is inactive (Carroll et al., 1996).

Previously, our laboratories identified five murine CYP2C cDNAs and found that each of the five CYP2C recombinant proteins metabolized AA with regiospecific product profiles and differential catalytic rates. A number of murine CYP2C cDNAs were detected by reverse transcriptase polymerase chain reaction (RT-PCR) in extrahepatic tissues (Luo et al., 1998). Preliminary studies in our laboratories indicate that the highest extrahepatic localization of CYP2Cs occurred in colon. Because little is known about the endogenous function of the CYP2Cs, we postulate that these enzymes may have important roles in the metabolism of physiologically important endogenous substrates such as AA. In this study, we found that CYP2Cs are highly expressed in proximal colon and cecum. The principal CYP enzyme in this tissue was identified as CYP2C40 and was found to metabolize AA into two mixtures of HETEs and EETs. Interestingly, the predominant product was 16(*R*)-HETE, an eicosanoid that has been shown to be vasoactive and inhibit adhesion and aggregation of neutrophils as an anti-inflammation strategy (Bednar et al., 1997, 1999). We also found CYP2C40 in peripheral cells of murine blood. This is the first enzyme shown to produce 16-HETE as the primary product and may act as a protective role in murine intestine. In addition, immunohistochemical studies showed that CYP2C40 is specifically localized to epithelial cells and autonomic ganglia in colon and gut, suggesting possible roles in absorption and gut motility.

Experimental Procedures

Materials. [1-^{14}C]AA was purchased from DuPont-NEN (Boston, MA). Midchain HETEs were purchased from Cayman Chemical (Ann Arbor, MI). EETs and 16-HETE were a generous gift from Dr. J. R. Falck. α-Bromo-2,3,4,5,6-pentafluorotolunen, *N*,*N*-diisopropyleneamine, diazald, 1-naphthoyl chloride, and pyridine were purchased from Aldrich Chemical Co. (Milwaukee, WI). All other chemicals and reagents were purchased from Sigma Chemical Co. (St. Louis, MO) unless otherwise specified.

Isolation of Total RNA and RT-PCR Analysis. Normal CD-1 female mouse intestinal tissues were snap-frozen in liquid nitrogen immediately after collection and stored at −80°C until use. Total RNA was extracted using Tri-Reagent (Molecular Research Center, Inc., Cincinnati, OH). RT-PCR analysis was performed using a GENEAmp RNA PCR kit (Perkin Elmer, Branchburg, NJ). Reverse transcription was performed with 1 μg of total RNA in a buffer containing 10 mM Tris-HCl (pH 8.3), 50 mM KCl, 5 mM $MgCl_2$, 2.5 mM oligo-dT primer, 1 mM each of dGTP, dATP, dTTP, and dCTP, and 50 U of Moloney murine leukemia virus-reverse transcriptase incubated at 42°C for 1 h. The PCR amplifications were performed in the presence of 2 mM $MgCl_2$, 0.1 mM forward and reverse primers (Table 1), using 2.5 U of AmpliTaq DNA polymerase. After an initial incubation at 95°C for 3 min, samples were subjected to 35 cycles of 30 s at 95°C, 30 s at 58°C, and 90 s at 72°C. The PCR products were electrophoresed on 1.2% agarose gels containing ethidium bromide. PCR products were also cloned into the pGEM vector using a PCR cloning kit from Promega (Madison, WI) for subsequent identification. DNA was prepared from selected clones and sequenced using an ABI Prism DNA sequencing kit (Perkin Elmer).

Protein Immunoblotting and Immunohistochemistry. Microsomal fractions were prepared from frozen normal CD-1 female intestinal tissues by differential centrifugation at 4°C as previously described (Zeldin et al., 1997). Polyclonal anti-mouse CYP2C38 IgG was raised in New Zealand White rabbits against the partially purified recombinant CYP2C38 protein and purified using a protein A column (Pierce, Rockford, IL) as previously described (Ma et al., 1999). For immunoblotting, microsomal fractions and partially purified recombinant proteins were electrophoresed in SDS-10% (w/v) polyacrylamide gels, and the resolved proteins were transferred onto nitrocellulose membranes. Membranes were immunoblotted using rabbit anti-mouse CYP2C38 IgG, goat anti-rabbit IgG conjugated to horseradish peroxidase (Amersham Life Sciences, Buckinghamshire, UK), and visualized using an ECL Western Blotting Detecting System (Amersham Life Sciences) as previously described (Zeldin et al., 1997).

For immunohistochemistry, specific regions of the small and large intestine were carefully collected and fixed in 10% neutral buffered formalin overnight (18–24 h), processed routinely, and embedded in paraffin. Localization of CYP2C protein expression was investigated using the anti-CYP2C38 IgG (1:1000 dilution) on serial 6 μM sections. Slides were deparaffinized in xylene and hydrated through a graded series of ethanol to 1X Automation buffer (Biomeda, Foster City, CA) washes. Endogenous peroxidase activity was blocked with 3% (v/v) hydrogen peroxide for 15 min. After rinsing in 1X Automation buffer, the sections were blocked with 5% normal goat serum for 20 min. All antibody incubations were carried out at room tempera-

TABLE 1
Designation of mouse CYP2C and β-actin genes primer sets for RT-PCR

Gene		Primer Sequence (5′–3′)	Product Size in Base Pairs
CYP2Cs	Forward	TCCATGCAATGTCATCTGCTC	826
	Reverse	GAATAGAAACAGCTCCATGCG	
CYP2C29	Forward	TCCATGCAATGTCATCTGCTC	548
	Reverse	GGACCTCATGAATCATGGCG	
CYP2C37	Forward	GATCGTTTTGATTATAAAGATCG	959
	Reverse	AACAAGCTTCTGCAGCCAGGCATTTGATTTTCGA	
CYP2C38	Forward	TCCATGCAATGTCATCTGCTC	991
	Reverse	ACCAAGCTTCTGCAGAATGTGTGATCTCTTTAG	
CYP2C39	Forward	TCCATGCAATGTCATCTGCTC	1013
	Reverse	AAGACCTGGACAGGATTGCAG	
CYP2C40	Forward	GCTCACCCTGTGATCCCCAATTCA	1051
	Reverse	TTGAGAAAAACAGCATAGCAG	
β-Actin	Forward	GAGCTATGAGCTGCCTGACG	409
	Reverse	CACTTGCGGTGCACGATG	

ture in a humidified chamber. The primary antibody, anti-CYP2C38 IgG, was applied, and sections were incubated for 1 h. Both preimmune IgG and rabbit nonimmune IgG (Jackson Immunoresearch, West Grove, PA) were used as the negative controls in place of the primary antibody, and mouse liver was used as positive control for immunostaining. The secondary antibody, biotinylated goat anti-rabbit IgG (Vector Laboratories, Burlingame, CA), was applied at a dilution of 1:600 for 30 min. The bound primary antibody was visualized by avidin-biotin-peroxidase detection using the Vectastain Rabbit Elite Kit (Vector Laboratories) according to the manufacturer's instructions with liquid diaminobenzidine (Dako Corp., Carpinteria, CA) as the color-developing reagent. Slides were counterstained with Harris hematoxylin, dehydrated through a graded series of ethanol to xylene washes, and cover-slipped with Permount (Fisher, Springfield, NJ). Slides were evaluated according to stain distribution, localization, and intensity. Stain intensity was scored as 1+, 2+, or 3+. Light brown stain above background was scored as 1+. Distinct brown staining was scored as 2+, and dark brown to black staining was scored as 3+.

Stereochemical Analysis of AA Metabolites of CYP2C40. The methods for expression, partial purification, and regiospecific metabolism of AA by the reconstituted recombinant protein CYP2C40 were previously described (Luo et al., 1998). For subsequent chiral analysis, the EETs were collected from high performance liquid chromatography (HPLC) eluent, derivatized to the corresponding EET-pentafluorobenzyl or EET-methyl esters, purified by normal phase HPLC, resolved into the corresponding antipodes by chiral-phase HPLC, and quantified by liquid scintillation as previously described (Hammonds et al., 1989; Capdevila et al., 1991). For regio- and stereochemistry of HETEs, a radiolabeled HPLC fraction that we previously identified as 16-, 17-, and/or 18-HETE (Luo et al. 1998) was collected from reverse-phase HPLC eluent and then rechromatographed on a normal-phase HPLC system to resolve individual HETE regioisomers as previously described (Rosolowsky and Campbell, 1996; Schlezinger et al., 1998). For chiral-phase chromatography, the CYP2C40-derived 16-HETE as well as standard samples of racemic 16-HETE, 16(*R*)-HETE, and 16(*S*)-HETE were methylated with diazomethane followed by treatment with 1-naphthoyl chloride as described (Oliw, 1990). The naphthoyl methyl ester derivatives were purified by a reverse-phase HPLC as described (Oliw, 1990). The separation of 16-HETE stereoisomers was accomplished with a Pirkle type 1-A column (5 μm, 250 $\times$ 4.6 mm; Regis Chemical Co., Morton Grove, IL) using hexane containing 0.25% of isopropanol at 1 ml/min as the mobile phase. Under these conditions, the retention time of 16(*R*)-HETE was 37 min, and that of 16(*S*)-HETE was 39 min. The effluent was analyzed by a UV detector and collected in fractions according to the UV peaks of 16(*R*)-HETE and 16(*S*)-HETE. The amount of radioactive material in the fractions was measured using a scintillation counter.

Incubations of Mouse Intestinal Microsomes with AA. Microsomal fractions were prepared from frozen mouse intestinal sections by differential centrifugation at 4°C, as described previously (Luo et al. 1998), and resuspended in 50 mM Tris-Cl, pH 7.4, 1 mM dithiothreitol, 1 mM EDTA, and 20% glycerol. Microsomal protein (3 mg/ml) was preincubated with shaking with 0.05 M Tris-Cl, pH 7.5, 0.15 M KCl, 0.01 M $MgCl_2$, 8 mM sodium isocitrate, 0.5 I.U./ml isocitrate dehydrogenase, and [1-^{14}C]AA (25–55 μCi/μmol; 50 μM final concentration) at 37°C for 5 min. After temperature equilibration, NADPH (1 mM final concentration) was added to initiate the reaction. Aliquots were withdrawn at 1 h intervals, and the reaction products were extracted into ethyl ether, dried under a stream of nitrogen, analyzed by reverse-phase HPLC, and quantified by online liquid scintillation counting using a Radiomatic Flow-One β-detector (Radiomatic Instruments, Tampa, FL) as described previously (Capdevila et al., 1991). Metabolites were identified by comparing their reverse-phase HPLC properties with those of authentic standards (Capdevila et al., 1991), and midchain HETE metabolites were identified by normal-phase HPLC as previously described (Rosolowsky and Campbell, 1996; Schlezinger et al., 1998).

Results

Screening of CYP2Cs in Intestinal Tract. Antibody to CYP2C38 recognized all five CYP2Cs and did not recognize other CYP subfamilies (Fig. 1, A and B). Preliminary data indicated that the highest extrahepatic distribution of CYP2Cs occurred in colon and cecum. In this study, we found that CYP2Cs were expressed throughout the intestinal tract, but the concentration was highest in cecum and colon (Fig. 1B). Interestingly, multiple polypeptide bands were found in upper intestinal tract, indicating the possibility that more than one CYP2C member exists in these tissues. However, the recombinant CYP2Cs had similar mobility on SDS-polyacrylamide gel electrophoresis, presumably because the N termini of several CYP2Cs were modified to maximize expression of the proteins in *Escherichia coli*. Attempts to make specific CYP2C peptide-based antibodies have been unsuccessful to date; thus we were unable to distinguish the individual CYP2Cs in the intestinal tract by immunoblotting. Therefore, RT-PCR cloning and sequencing of PCR products were performed as an alternative method to achieve this

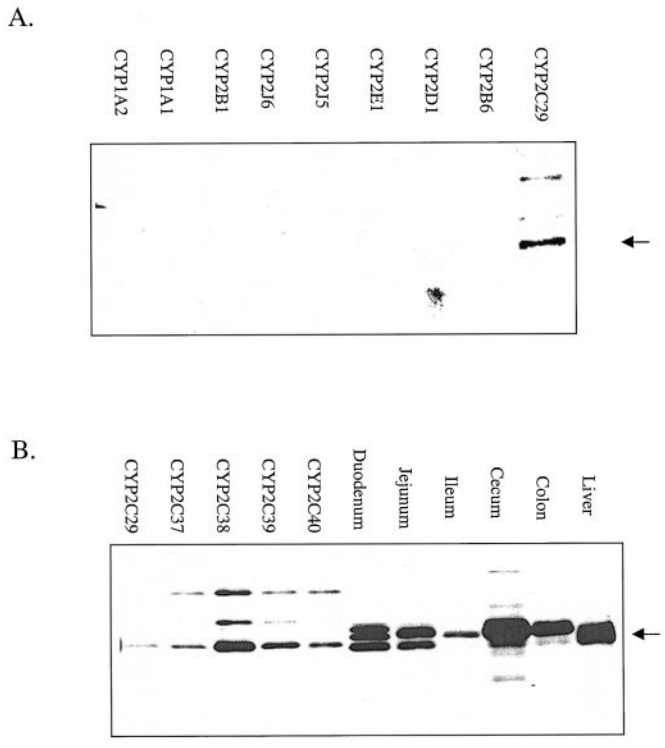

Fig. 1. Intestinal distribution of murine CYP2C proteins by immunobloting. A, partially purified recombinant CYP2C29 (0.01 pmol/lane); purified CYP2B6, CYP2D1, CYP2E1, CYP2B1, CYP1A1, and CYP1A2 (0.2 pmol/lane); and microsomal fractions prepared from *Sf*9 cells CYP2J5 and CYP2J6 (0.2 pmol/lane) were electrophoresed on SDS-10% polyacrylamide gel, transferred to nitrocellulose, and immunoblotted with the anti-CYP2C38 antibody as described under *Experimental Procedures*. B, partially purified recombinant CYP2C29, CYP2C37, CYP2C38, CYP2C39, and CYP2C40 (0.05 pmol/lane) and microsomal fractions prepared from mouse liver (1 μg), duodenum, jejunum, ileum, cecum, and colon (20 μg/lane) were electrophoresed on 10% SDS-polyacrylamide gels, and resolved proteins were transferred to nitrocellulose membranes. The membrane was immunoblotted using murine CYP2C38 antiserum which recognized all five murine CYP2Cs. The immunoreactive proteins were visualized using the ECL detection system and autoradiography.

purpose. To ensure the quality and integrity of RNA preparations, tissue samples were first analyzed for the presence of β-actin transcripts. All samples had similar expression levels of β-actin mRNA (Fig. 2A). Using primers to conserved regions in all mouse CYP2Cs, we were able to amplify 826-base pair CYP2C fragments from selected mouse intestinal tract sections (Fig. 2B). CYP2C mRNAs were most abundant in colon, which is consistent with the results of Western blot in Fig. 1B. The PCR products of each intestinal section were further cloned into pGEM vectors, and individual positive clones were selected for sequence determination. Sequence analysis indicates that all PCR clones are CYP2C40 in each region of the mouse intestinal tract (Table 2).

RT-PCR reactions with sequence-specific primers to amplify CYP2C29, CYP2C37, CYP2C38, CYP2C39, and CYP2C40 cDNAs were also performed. CYP2C40 mRNA was expressed throughout the entire intestinal tract (Fig. 2G). CYP2C29 mRNA was also present in duodenum and jejunum (Fig. 2C). CYP2C38 mRNA was present in duodenum and traces throughout the intestinal tract, except for colon (Fig. 2E). CYP2C37 and CYP2C39 mRNAs were not found in the intestinal tract (Fig. 2, D and F). Correlation of this data with immunoblotting results suggests that the large band with intermedial mobility on blots probably represents CYP2C40, whereas the lower bands in jejunum most likely represent CYP2C29 (Figs. 1B and 2).

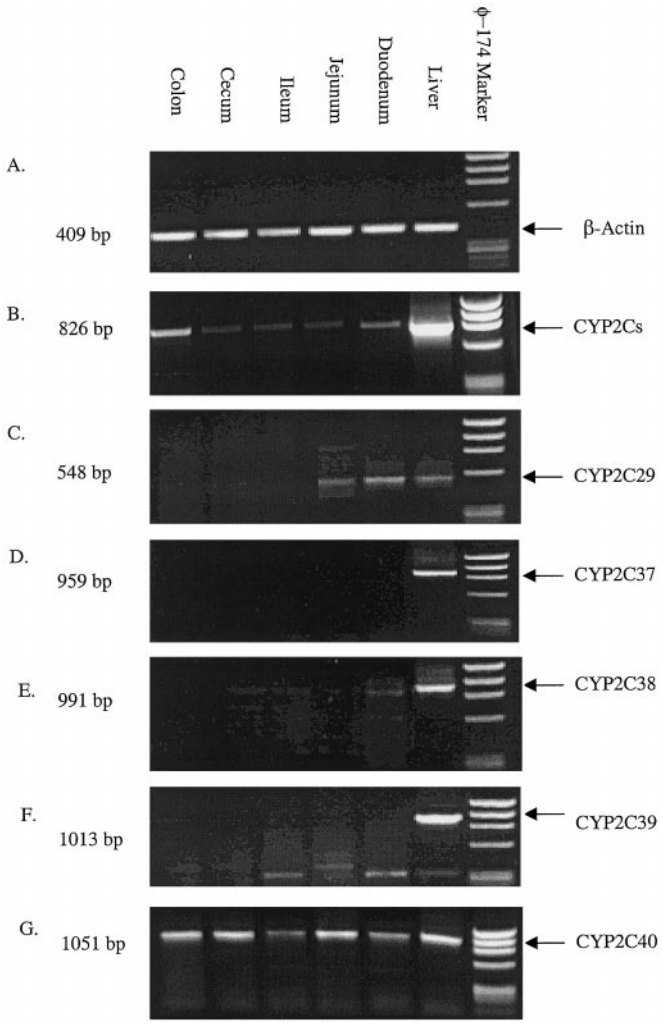

Fig. 2. Detection of mRNA of the murine CYP2Cs in tissues by RT-PCR. Total RNA extracted from female murine liver, duodenum, jejunum, ileum, cecum, and colon was used to synthesize cDNAs using Moloney murine leukemia virus reverse transcriptase and amplified by PCR using primer sets for β-actin (A), CYP2Cs (B), CYP2C29 (C), CYP2C37 (D), CYP2C38 (E), CYP2C39 (F), and CYP2C40 (G). PCR products (10 μl) were electrophoresed on 1.5% agarose gels and analyzed using ethidium bromide staining.

Localization of Intestinal CYP2C Proteins by Immunohistochemistry. Immunohistochemical localizations of CYP2C proteins were examined in the small and large intestines of mice using a polyclonal antibody to CYP2C38 that recognizes all five known murine CYP2Cs. In small intestine, staining was localized to the cytoplasm of the villi epithelium at varying intensities. In duodenum, the majority of villi epithelium stained at an intensity of 2+ (Fig. 3A), whereas in the jejunum and ileum, the number of stained cells decreased significantly and, of those staining, the intensity was 1+ (Fig. 3, B and C). However, the distribution and intensity of staining increased to 3+ in the cecum (Fig. 3D). This pattern of intense staining continued in the proximal colon (Fig. 3E) and gradually decreased distally (Fig. 3F). In addition, staining was localized in ganglia with 1+ intensity in proximal colon (Fig. 3E).

In Vitro Metabolism of AA by Recombinant CYP2C40. Incubations of partially purified recombinant CYP2C40 proteins reconstituted with NADPH-P450 oxido/reductase and dilauroylphosphatidylcholine, followed by the addition of [1-^{14}C]AA and NADPH, resulted in the formation of EETs and HETEs (Fig. 4A). These metabolites were tentatively identified by comparing their RP-HPLC properties with those of authentic standards. CYP2C40 metabolized AA to 14,15-, 11,12-, and 8,9-EETs, and a fraction containing that coeluted with 16-, 17-, and 18-HETEs (Luo et al., 1998). To determine the identity of HETEs found in this fraction, it was collected batchwise and rechromatographed in this study on a normal phase HPLC system that can separate 16-, 17-, and 18-HETEs. We found that only 16-HETE was present in this fraction (Fig. 4B). Thus, CYP2C40 metabolized AA into the metabolites in the following order: 16-HETE > 14,15-EET ≫ 8,9-EET > 11,12-EET. To determine the stereoselectivity of AA metabolites produced by CYP2C40, the fractions containing 16-HETE, 14,15-EET, 11,12-EET, and 8,9-EET were collected, derivatized, and further resolved by chiral-phase HPLC to distinguish the individual enantiomers (Fig. 5). CYP2C40 produced EETs and 16-HETE in a moderate stereoselective manner with preference for 16(*R*)-HETE (66%) (Fig. 5), 14(*R*),15(*S*)-EET (62%), 11(*S*),12(*R*)-EET (70%), and 8(*S*),9(*R*)-EET (86%) (Table 3).

Characterization of Intestinal CYP-AA Metabolism. To examine the differences in CYP metabolism of AA among

TABLE 2

Sequence analysis of CYP2Cs in murine intestinal tract sections

RT-PCR was performed using total RNA from murine intestinal tract sections using universal CYP2C primer set. The PCR products were cloned into pGEM vectors using a TA cloning kit (Promega, Madison, WI). Plasmids were prepared from the positive colonies, and their sequences were determined.

Tissues	cDNAs Found in Clones
Small intestine	CYP2C40 (8/8)
Duodenum	CYP2C40 (8/8)
Jejunum	CYP2C40 (9/9)
Ileum	CYP2C40 (8/8)
Cecum	CYP2C40 (10/10)
Colon	CYP2C40 (12/12)

mouse intestinal tract, microsomal fractions prepared from murine jejunum, cecum, and colon were incubated with [1-^{14}C]AA in the presence of NADPH, and the organic soluble metabolites were resolved by reverse-phase HPLC. Murine cecum exhibited the highest conversion rate (14.6 pmol/mg/min), whereas the rate of colon was 8.4 pmol/mg/min, and jejunum had the lowest turnover number (3.41 pmol/mg/min). Comparing the HPLC profiles of AA metabolites, an additional peak coeluting with 16-, 17-, 18-, and 20-HETE was found in cecum and colon but was not observed in jejunum (Fig. 6). Metabolites of midchain HETE fractions from cecum and colon were collected and applied to normal-phase HPLC to distinguish the midchain HETE metabolites. Cecum and colon microsomes metabolized AA into distinctly different HETE metabolites (Table 4). The major HETE produced by cecum is 19-HETE, whereas the principal metabolite in colon is 20-HETE. However, significant amounts of 16-HETE were produced by cecum, which has the highest expression of CYP2C proteins, but this metabolite was below the limits of detection in colon, perhaps because the CYP2Cs are not seen throughout this tissue.

Discussion

This study shows CYP2C40 is expressed throughout the entire gastrointestinal tract with the highest concentrations in cecum and proximal colon. It is localized to specific cell types within the intestine, namely epithelial cells and autonomic ganglial cells. In addition, CYP2C40 metabolizes AA in vitro to 16-HETE and EETs in a stereoselective manner. To our knowledge, CYP2C40 is the first enzyme found to produce 16(*R*)-HETE as the major product of AA. This unique metabolite and the expression of CYP2C40 in the intestinal tract suggest that CYP2C40 could have important biological functions in murine intestine through the production of 16(*R*)-HETE.

Previous studies showed that a number of CYPs are constitutively expressed in rat, mouse, and human intestine, including members of the CYP1A, CYP2B, CYP2C, CYP2D, CYP2E, CYP2J, and CYP3A subfamilies (Watkins et al., 1987; Murray et al., 1988; Peters et al., 1989; Rich et al., 1989; de Waziers et al., 1990; Shimizu et al., 1990; Fasco et al., 1993; Zeldin et al., 1997; Dey et al., 1999). CYP proteins were expressed at the highest concentration in the proximal small intestine and decreased distally, with the lowest concentration in the colon. In contrast, some CYP enzymes, such as CYP2Js and CYP3A4, were found to be uniformly expressed throughout the entire gastrointestinal tract at similar levels (de Waziers et al., 1990; Zeldin et al., 1997). In the mouse, CYP2C isoforms are expressed throughout the intestinal tract but have higher expression levels in cecum and colon. We used universal CYP2C primers for RT-PCR cloning and subsequent sequencing of individual PCR clones to identify the particular CYP2Cs expressed in mouse intestinal tract. Interestingly, all the selected clones had sequences that were identical with CYP2C40. We also found small amounts of CYP2C29 and CYP2C38 in duodenum by RT-PCR using specific primers. These data suggest CYP2C40 is the most abundant CYP2C in intestine, but that CYP2C29 and CYP2C38 are also present in murine intestine, primarily in duodenum.

The intestinal localization of CYP2Cs was evaluated by immunohistochemistry. CYP2Cs were expressed principally in epithelial cells of the intestinal tract and had the highest expression in cecum and proximal colon. Transport of fluids and electrolytes from the intestinal lumen is one of the major

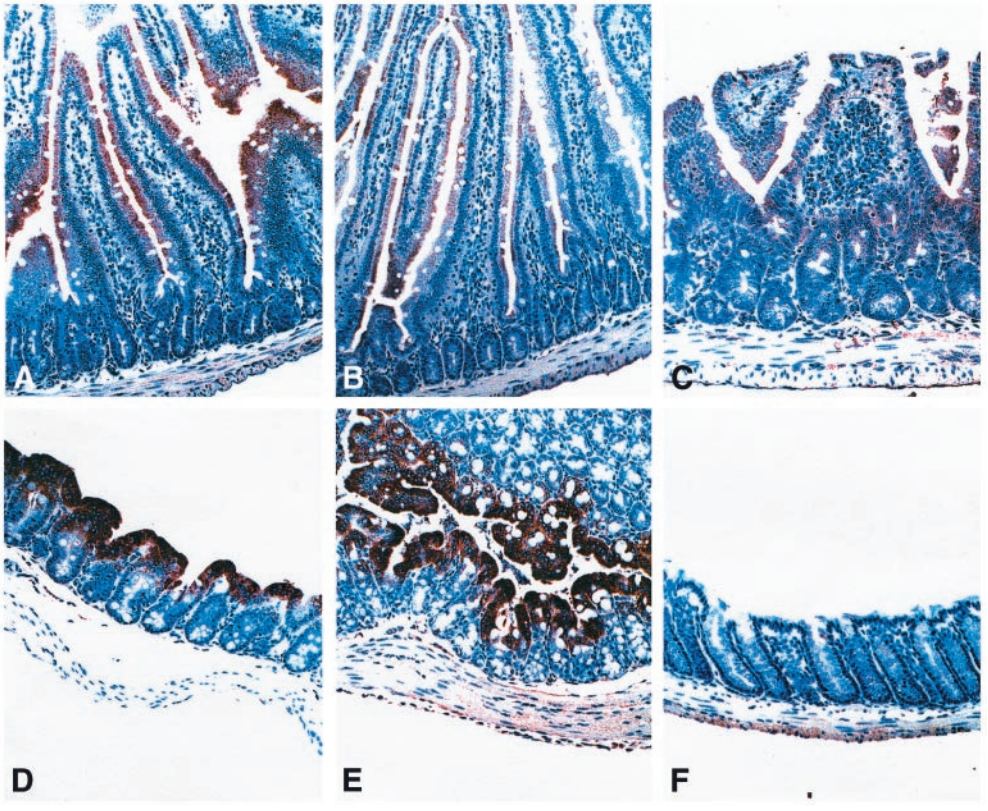

Fig. 3. Immunohistochemical staining of CYP2C proteins in the small and large intestine. A, duodenum. Positive staining is localized to the epithelium of villi and ganglia (not shown in this slide). B, jejunum. Positive staining is localized to the epithelium of villi; however, the number of cells that stained and the intensity of the stain decreased relative to the duodenum. C, only trace staining of CYP2C proteins was observed in the ileum. Strong positive staining was observed in the luminal epithelium in the cecum (D) and in the proximal colon (E). Only traces of staining for CYP2C proteins were observed in distal colon (F).

functions of epithelial cells of colon. The abundant expression of CYP2C40 in epithelial cells of cecum and colon suggests that products of this enzyme may have endogenous biological activity related to fluid/electrolyte transport in gut. It has been argued that mammalian colon cannot be regarded as a single organ with electrolyte transport processes distributed uniformly throughout its length (Clauss et al., 1985). Distinct differences in the mechanisms of electrolyte transport have been demonstrated between the proximal and distal colon in a variety of species (Yau and Makhlouf, 1975). For example, it has been found that rat proximal colon absorbed significantly more Na^+ and secreted significantly less HCO_3^- than descending colon, whereas only the descending colon absorbed K^+ (Yau and Makhlouf, 1975). The fact that CYP2C40 is present in the highest concentration in the proximal colon and expression decreased along the distal colon suggests that the biological activity of CYP2C40 products could be related to differential water and/or electrolyte transport in murine intestinal tract.

AA metabolites have been reported in epithelial cells where they have been suggested to affect transepithelial electroytes and water transportation in cells (Douglas et al., 1990; Carroll et al., 1991; Hill et al., 1992). In rabbit kidney, HETEs have been shown to affect electrolyte transport (Carroll et al., 1991). 16(*R*)-HETE was found to have effects on renal vasodilation, whereas its enantiomer, 16(*S*)-HETE, has negligible vasoactivity but can inhibit proximal tubular Na^+/K^+-ATPase (Carroll et al., 1996). EETs have been found to alter cellular Ca^{2+} concentrations (Kutsky et al., 1983) and affect vascular smooth muscle tone in intestine and other extrahepatic tissues (Proctor et al., 1987). Furthermore, a recent study demonstrated that 14,15-EET stimulated phosphatidylinositol (PI) 3-kinase in mitogenic pathways (Chen et al., 1998, 1999). It has been hypothesized that PI 3-kinase may mediate the inhibitory effect of epidermal growth factor on calcium-dependent chloride secretion in colonic cells (Uribe et al., 1996). Moreover, PI 3-kinase was reported to stimulate Na^+/H^+ exchange activity and NaCl absorption in intestinal epithelial cells (Khurana et al., 1996). Therefore, it

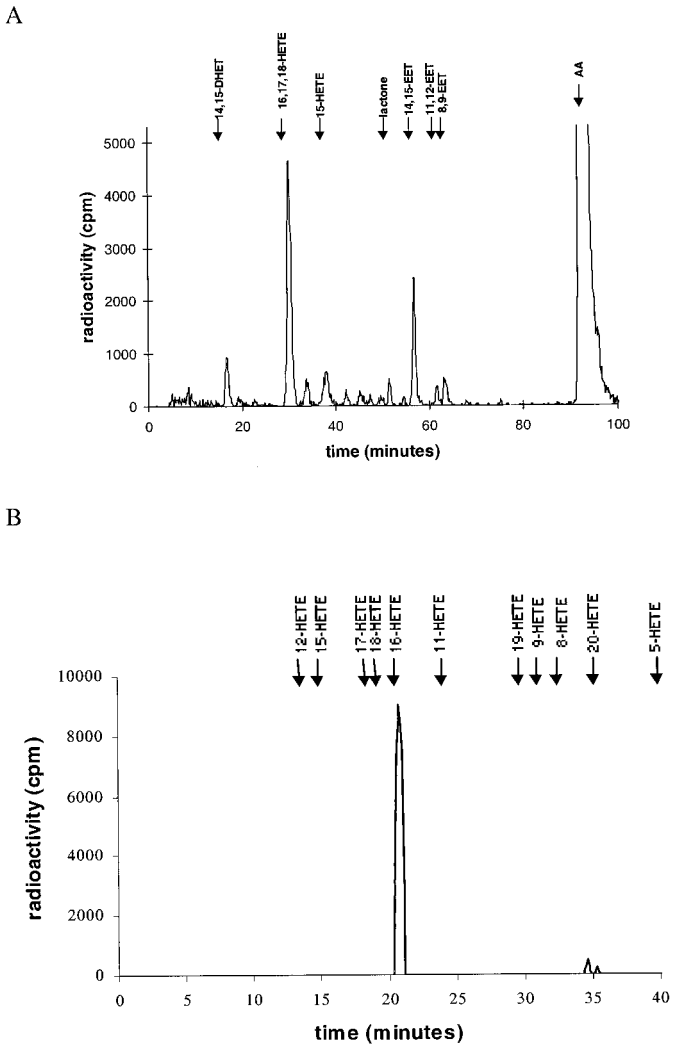

Fig. 4. HPLC profiles of metabolism of arachidonic acid by murine CYP2C40. A, 140 pmol of CYP2C40 was used for each reaction. The organic soluble products were extracted immediately into ethyl ether, dried under a nitrogen stream, resolved by reverse-phase HPLC, and quantified by on-line liquid scintillation using a Radiomatic Flow-One β-detector. The retention times of authentic standards are indicated by the arrows above the respective peaks. B, the fraction eluants collected each minute were resolved by normal phase HPLC as described under *Experimental Procedures*. The HETE metabolites were quantified by a Radiomatic Flow-One β-detector. The retention times of authentic standards are indicated by the arrows above.

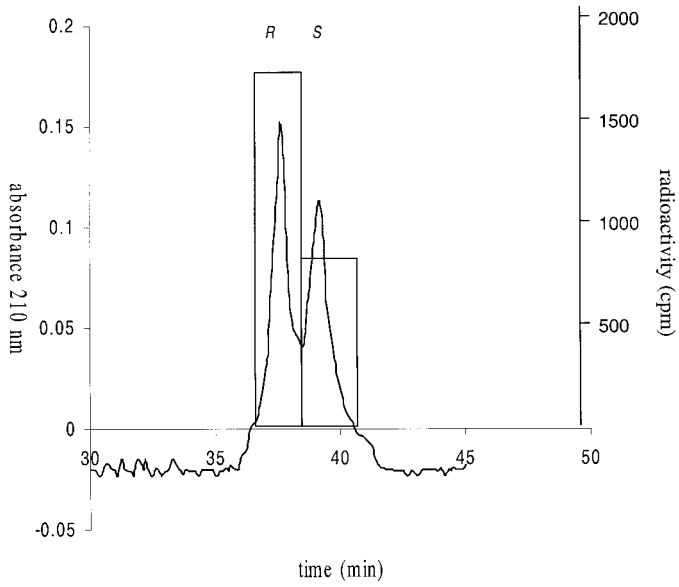

Fig. 5. Chiral-phase HPLC of 16-HETE metabolized by CYP2C40 mixed with racemic 16-HETE standards and analyzed as naphthoyl methyl ester. The bars represent the total amount of the radioactivity in the fractions collected according to the UV peaks of 16(*R*)-HETE and 16(*S*)-HETE.

TABLE 3

Regio- and enantioselective composition of HETEs and EETs produced by recombinant CYP2C40

The regio- and stereochemical composition of EETs formed by incubation of recombinant CYP2C40 with [1-^{14}C]AA were quantified by HPLC and liquid scintillation as described under *Experimental Procedures*. Values shown were averages of at least three different experiments with standard errors less than 5%.

Regioisomer	Distribution	Enantioselectivity	
		R,S	*S,R*
	%	%	
14,15-EET	34	62	38
11,12-EET	3	30	70
8,9-EET	4	14	86
16-HETE	57	66 (*R*)	34 (*S*)

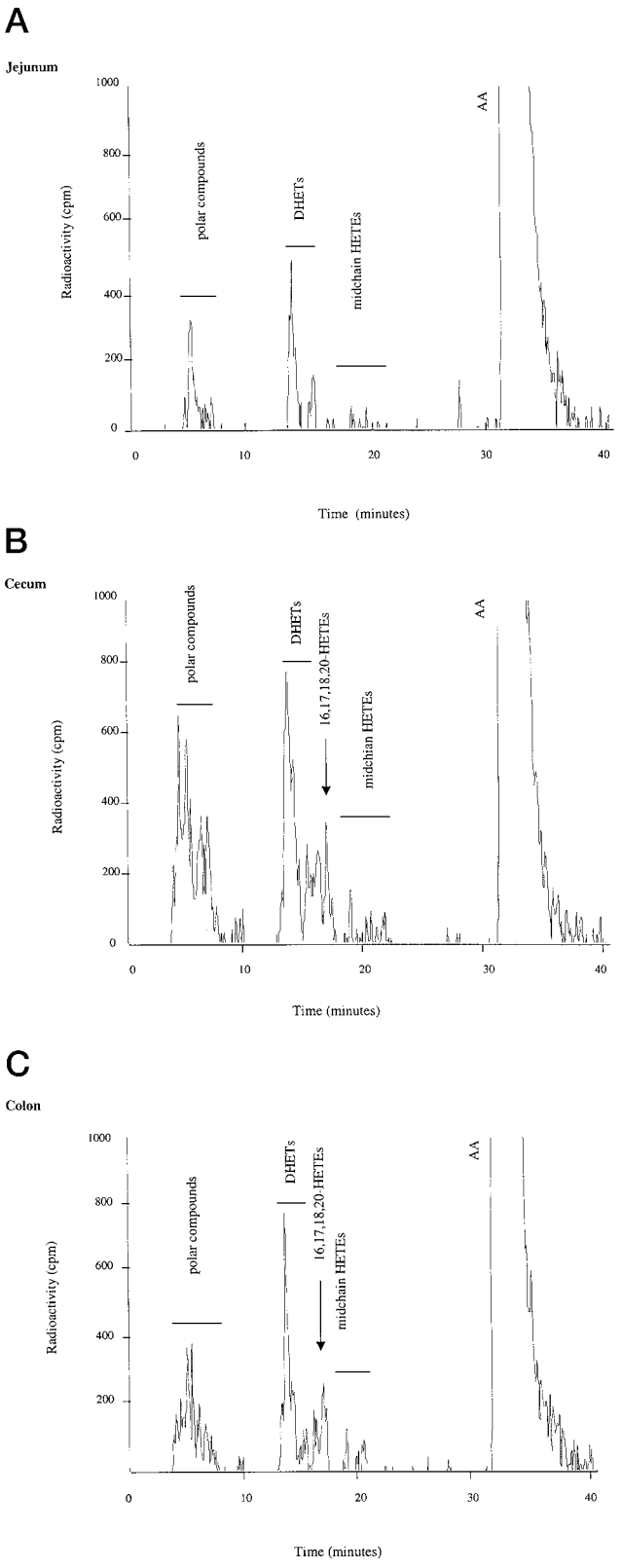

Fig. 6. HPLC profiles of metabolism of arachidonic acid by murine intestinal microsomes. Murine jejunum (A), cecum (B), and colon (C) microsomal proteins (3 mg/ml each) were used for the reaction. The organic soluble products were extracted immediately into ethyl ether, dried under nitrogen stream, resolved by reverse-phase HPLC, and quantified by on-line liquid scintillation using a Radiomatic Flow-One β-detector. The retention times of authentic standards are indicated by the arrows above the respective peaks.

is possible that 14,15-EET may modulate transport functions in a variety of epithelial cells.

CYP-AA metabolism throughout the murine intestinal tract was also characterized in this study. Although 19-HETE was the most abundant HETE metabolite produced by murine cecum microsomes, significant amounts of 16-HETE were also produced. Other CYPs such as CYP2E1 and CYP2Js, which produce 19-HETE as the major AA metabolites, have been reported in intestinal tract (Laethem et al., 1993; Zeldin et al., 1997); however, these CYPs do not convert AA to 16-HETE. Rabbit ileal microsomes have also been reported to form 16-HETE (Macica et al., 1993). In this study, 16-HETE was only detected in murine cecum. The expression of CYPs in intestinal tract is far less than in liver, and the relative amounts of members of CYP2Cs could limit the detection of individual HETE metabolites by the murine intestinal tract. The fact that CYP2C40 has the highest expression in cecum and 16-HETE was only detected in AA metabolites of murine cecum microsomes is consistent with the hypothesis that CYP2C40 is the enzyme in intestine that produces 16-HETE.

In addition to epithelial cells, we found CYP2C proteins in nerve cells of autonomic ganglia, suggesting that AA metabolites of CYP2C40 could have a role in intestinal neurotransmission and control of gut motility. EETs have been reported to stimulate the release of somatostatin and other neuropeptides (Ojeda et al., 1989), suggesting a role of these eicosanoids in mediating the effects of intestinal neurotransmitters and controlling gut motility. CYP2C proteins are localized in ganglionic cells of colon and intestine and are capable of metabolizing AA to EETs, which suggests a possible involvement of CYP2C in colonal and intestinal motility.

Human neutrophils have been found to produce 16(*R*)-HETE, which functions as a modulator of neutrophil activity by inhibiting neutrophil adhesion and aggregation (Bednar et al., 1997, 2000). It is well documented that neutrophils play an important role in the pathogenesis of inflammatory bowel diseases such as ulcerative colitis, Crohn's disease, and bacterial entercolitis (Kumar et al., 1982; Teahon et al., 1991). Neutrophils are also a central component in intestinal dysfunction after ischemic injury and largely responsible for subsequent increased mucosal permeability and fluid loss into the lumen (Parkos, 1997). In many inflammatory condi-

TABLE 4

Regioselective composition of HETEs produced by murine cecum and colon microsomes

The regiochemical of HETEs formed by incubation of cecum and colon microsomes with [1-^{14}C]AA were quantified by HPLC and liquid scintillation as described under *Experimental Procedures*.

Regioisomer	Distribution	
	Cecum	Colon
	%	
8-HETE	N.D.	14.8
9-HETE	9.2	3.2
11-HETE	N.D.	16.1
12-HETE	20.5	3.6
15-HETE	3.6	6.4
16-HETE	8.8	N.D.
18-HETE	N.D.	5.1
19-HETE	54.7	3.3
20-HETE	3.2	47.5

N.D., nondetectable.

tions of the intestinal tract, patient disease symptoms correlate with the adhesion of neutrophils on epithelial cells and migration of neutrophils across gut epithelium (Parkos, 1997). These findings lead us to hypothesize that CYP2C40 may have a protective role in the murine intestinal tract by producing 16(*R*)-HETE, which inhibits the adhesion and aggregation of neutrophils to protect the gut from diseases and injuries.

Furthermore, the fact that CYP2C40 is the first protein found to produce 16(*R*)-HETE suggests the possibility that murine neutrophils contain CYP2C40. Results of RT-PCR and immunoblotting indicated that CYP2C40 mRNAs and a CYP2C protein band with the same molecular weight as CYP2C40 were present in the murine peripheral blood cells enriched for neutrophils (our unpublished data). These findings suggest that CYP2C40 may have an important role in anti-inflammation processes. Interestingly, PCR with universal CYP2C primers followed by subcloning and sequence analysis indicated that CYP2C37 is the major murine CYP2C in peripheral cells (9/10 clones), although one selected clone was CYP2C40. However, this fraction still contained platelets, which are presumably the source of CYP2C37. A previous study (Luo et al., 1998) showed that 12-HETE is the major AA metabolite produced by CYP2C37, and many studies suggested that 12-HETE production in platelets is important in anti-inflammatory processes (Lianos and Bresnahan, 1999). Our findings suggest that CYP2C40 and CYP2C37 isoforms may exist in different types of blood cells and have important anti-inflammatory roles.

In summary, molecular and immunological data show that CYP2C proteins are abundantly expressed in the murine intestinal tract. CYP2C40 has been shown to be the major CYP2C in the mouse intestinal tract. We also report the regio- and stereospecificity for CYP2C40 AA metabolites. Moreover, CYP2C40 is capable of metabolizing AA to a unique product, 16(*R*)-HETE, as well as EETs. Our data show that CYP2C40 is the major CYP2C in gut, particularly in colon, and it produces unique AA metabolites that may have important effects on physiological functions such as intestinal fluid/electrolyte transport, control of intestinal motility, and anti-inflammation. Future studies will address the functional significance of CYP2C40 in gastrointestinal physiology and pathology.

Acknowledgments

We thank Masahiko Negishi, Joyce Blaisdell, Chandrashekhar Joshi, and Diana Dai for helpful comments during the preparation of this manuscript.

References

Bednar MM, Gross CE, Balazy M and Falck JR (1997) Antineutrophil strategies. *Neurology* **49:**S20–S22.

Bednar MM, Gross CE, Balazy MK, Belosludtsev Y, Cloella DT, Falck JR and Balazy M (2000) 16(*R*)-Hydroxy-5,8,11,14-eicosatetraenoic acid, a new arachidonate metabolite in human polymorphonuclear leukocytes. *Biochem Pharmacol* **60:**447–455.

Capdevila J, Chacos N, Werringloer J, Prough RA and Estabrook RW (1981) Liver microsomal cytochrome P-450 and the oxidative metabolism of arachidonic acid. *Proc Natl Acad Sci USA* **78:**7375–7378.

Capdevila JH, Dishman E, Karara A and Falck JR (1991) Cytochrome P450 arachidonic acid epoxygenase: Stereochemical characterization of epoxyeicosatrienoic acids. *Methods Enzymol* **206:**441–453.

Capdevila JH, Falck JR and Estabrook RW (1992) Cytochrome P450 and the arachidonate cascade. *FASEB J* **6:**731–736.

Carroll MA, Balazy M, Margiotta P, Huang D-D, Falck JR and McGiff JC (1996) Cytochrome *P-450*-dependent HETEs: Profile of biological activity and stimulation by vasoactive peptides. *Am J Physiol* **271:**R863–R869.

Carroll MA, Sala A, Dunn CE, McGiff JC and Murphy RC (1991) Structural identification of cytochrome P450-dependent arachidonate metabolites formed by rabbit medullary thick ascending limb cells. *J Biol Chem* **266:**12306–12312.

Chen J-K, Falck JR, Reddy KM, Capdevila J and Harris RC (1998) Epoxyeicosatrienoic acids and their sulfonimide derivatives stimulate tyrosine phosphorylation and induce mitogenesis in renal epithelial cells. *J Biol Chem* **273:**29254–29261.

Chen JK, Wang DW, Falck JR, Capdevila J and Harris RC (1999) Transfection of an active cytochrome P450 arachidonic acid epoxygenase indicates that 14, 15-epoxyeicosatrienoic acid functions as an intracellular second messenger in response to epidermal growth factor. *J Biol Chem* **274:**4764–4769.

Clauss W, Schafer H, Horch I and Hornicke H (1985) Segmental differences in electrical properties and Na-transport of rabbit cecum, proximal and distal colon *in vitro*. *Pfluegers Arch* **403:**278–282.

de Waziers I, Cugnenc PH, Yang CS, Leroux J-P and Beaune PH (1990) Cytochrome P450 isoenzymes, epoxide hydrolase and glutathione transferases in rat and human hepatic and extrahepatic tissues. *J Pharmacol Exp Ther* **253:**387–394.

Dey A, Jones JE and Nebert DW (1999) Tissue- and cell type-specific expression of cytochrome P450 1A1 and cytochrome P450 1A2 mRNA in the mouse localized *in situ* hybridization. *Biochem Pharmacol* **58:**525–537.

Douglas JC, Romero M and Hopfer U (1990) Signaling mechanisms coupled to the angiotensin receptor of proximal tubular epithelium. *Kidney Int* **38 (Suppl 30):** S43–S47.

Fasco MJ, Silkworth JB, Dunbar DA and Kaminsky LS (1993) Rat small intestinal cytochrome P450 probed by warfarin metabolism. *Mol Pharmacol* **43:**226–233.

Hammonds TD, Blair IA, Falck JR and Capdevila JH (1989) Resolution of epoxyeicosatrienoate enantiomers by chiral phase chromatography. *Anal Biochem* **182:** 300–303.

Hill E, Fitzpatrick F and Murphy RC (1992) Biological activity and metabolism of 20-hydroxyeicosatetraenoic acid in human platelet. *Br J Pharmacol* **106:**267–274.

Kaminsky LS and Fasco MJ (1992) Small intestinal cytochrome P450. *Crit Rev Toxicol* **21:**407–422.

Khurana S, Nath SK, Levine SA, Bowser JM, Tse CM, Cohen ME and Donowitz M (1996) Brush border phosphatidylinositol 3-kinase mediates epidermal growth factor stimulation of intestinal NaCl absorption and Na^+/H^+ exchange. *J Biol Chem* **271:**9919–9927.

Kumar NB, Nostrant TT and Appelman HD (1982) The histopathologic spectrum of acute self-limited colitis (acute infectious type colitis). *Am J Surg Pathol* **6:**523–529.

Kutsky P, Falck JR, Weiss GB, Manna S, Chacos N and Capdevila J (1983) Effects of newly reported arachidonic acid metabolites on microsomal Ca^{2+} binding, uptake, and release. *Prostaglandins* **26:**13–21.

Laethem RM, Balazy M, Falck JR, Laethem CM and Koop DR (1993) Formation of 19(S)-, 19 (R)-, and 18(R)-hydroxyeicosatetraenoic acids by alcohol-inducible cytochrome P450 2E1. *J Biol Chem* **268:**12912–12918.

Lianos EA and Bresnahan BA (1999) Effect of thromboxane A2 inhibition and antagonism on prostaglandin and leukotriene synthesis in glomerular immune injury. *J Lab Clin Med* **134:**478–482.

Luo G, Zeldin DC, Blaisdell JA, Hodgson E and Goldstein JA (1998) Cloning and expression of murine CYP2Cs and their ability to metabolize arachidonic acid. *Arch Biochem Biophys* **357:**45–97.

Ma J, Qu W, Scarborough PE, Tomer KB, Moomaw CR, Maronpot R, Davis LS, Breyer MD and Zeldin DC (1999) Molecular cloning, enzymatic characterization, developmental expression, and cellular localization of a mouse cytochrome P450 highly expressed in kidney. *J Biol Chem* **274:**17777–17788.

Macica C, Balazy M, Falck JR, Mioskowski C and Carroll MA (1993) Characterization of cytochrome *P*-450-dependent arachidonic acid metabolism in rabbit intestine. *Am J Physiol* **28:**G735–G741.

McGiff JC (1991) Cytochrome P450 metabolism of arachidonic acid. *Annu Rev Pharmacol Toxicol* **31:**339–369.

Murray GI, Barnes TS, Sewell HF, Ewen SW, Melvin WT and Burke MD (1988) The immunocytochemical localisation and distribution of cytochrome P-450 in normal human hepatic and extrahepatic tissues with a monoclonal antibody to human cytochrome P-450. *Br J Clin Pharmacol* **25:**465–475.

Ojeda SR, Urbanski HF, Junier M-P and Capdevila J (1989) The role of arachidonic acid and its metabolites in the release of neuropeptides. *Ann NY Acad Sci* **559:** 192–207.

Oliw EH (1990) Resolution of enantiomers of 19-hydroxyeicosatetraenoate and 18-hydroxyeicosatetraenoate by chiral phase high-performance liquid chromatograph of naphthoyl ester derivatives. *J Chromatogr* **526:**525–529.

Oliw EH, Guengerich FP and Oates JA (1982) Oxygenation of arachidonic acid by hepatic monooxygenases. Isolation and metabolism of four epoxide intermediates. *J Biol Chem* **257:**3771–3781.

Parkos CA (1997) Cell adhesion and migration I. Neutrophil adhesive interactions with intestinal epithelium. *Am J Physiol* **273:**G763–G768.

Peters WHM and Kremers PG (1989) Cytochromes P450 in the intestinal mucosa of man. *Biochem Pharmacol* **38:**1535–1538.

Proctor K, Falck J and Capdevila J (1987) Intestinal vasodilation by epoxyeicosatrienoic acids: Arachidonic acid metabolites produced by a cytochrome P450 monooxygenase. *Circ Res* **60:**50–59.

Rich KJ, Sesardic D, Foster JR, Davies DS and Boobis AR (1989) Immunohistochemical localization of cytochrome P450b/e in hepatic and extrahepatic tissues of the rat. *Biochem Pharmacol* **38:**3305–3322.

Rosolowsky M and Campbell WB (1996) Synthesis of hydroxyeicosatetraenoic (HETEs) and epoxyeicosatrienoic acids (EETs) by cultured bovine coronary artery endothelial cells. *Biochim Biophys Acta* **1299**:267–277.

Schlezinger JJ, Parker C, Zeldin DC and Stegeman JJ (1998) Arachidonic acid metabolism in the marine fish *Stenotomus chrysops* (Scup) and the effects of cytochrome P450 1A inducers. *Arch Biochem Biophys* **15:**265–275.

Shimizu M, Lasker JM, Tsutsumi M and Lieber CS (1990) Immunohistochemical

localization of ethanol-inducible P450IIE1 in the rat alimentary tract. *Gastroenterology* **99:**1044–1053.
Teahon K, Smethurst P, Pearson M, Levi AJ and Bjarnason I (1991) The effect of elemental diet on intestinal permeability and inflammation in Crohn's disease. *Gastroenterology* **101:**84–89.
Uribe JM, Keely SJ, Traynor-Kaplan AE and Barrett KE (1996) Phosphatidylinositol 3-kinase mediates the inhibitory effect of epidermal growth factor on calcium-dependent chloride secretion. *J Biol Chem* **271:**26588–26595.
Watkins PBS, Wrighton SA, Schuetz EG, Molowa DT and Guzelian PS (1987) Identification of glucocorticoid-inducible cytochrome P450 in the intestinal muscosa of rats and man. *J Clin Invest* **80:**1029–1036.
Whittle BJR and Vane JR (1989) Prostanoids as regulators of gastrointestinal function, in *Physiology of the Gastrointestinal Tract,* 2nd ed (Johnson LR ed) pp 143–180, Raven Press, New York.
Yau WM and Makhlouf G (1975) Comparison of transport mechanisms in isolated ascending and descending rat colon. *Am J Physiol* **228:**191–195.
Zeldin DC, Foley J, Goldworthy SM, Cook ME, Boyle JE, Ma J, Moomaw CR, Tomer KB, Steenbergen C and Wu S (1997) CYP2J subfamily cytochrome P450s in the gastrointestinal tract: Expression, localization, and potential functional significance. *Mol Pharmocol* **51:**931–943.
Zhang Q-Y, Raner G, Ding X, Dunbar D, Coon MJ and Kaminsky LS (1998) Characterization of the cytochrome P450 CYP2J4: Expression in rat small intestine and role in retinoic acid biotransformation from retinal. *Arch Biochem Biophys* **353:** 257–264.

Send reprint requests to: Dr. Joyce A. Goldstein, Laboratory of Pharmacology and Chemistry, National Institute of Environmental Health Sciences, 111 T.W. Alexander Dr., Research Triangle Park, NC 27709. E-mail: goldste1@niehs.nih.gov